CrossMark

ORIGINAL ARTICLE

Sclerostin does not play a major role in the pathogenesis of skeletal complications in type 2 diabetes mellitus

M. Pereira[1] · S. Gohin[1] · N. Lund[1] · A. Hvid[1] · P. J. Smitham[2,4] · M. J. Oddy[3] ·
I. Reichert[5] · D. Farlay[6] · J. P. Roux[6] · M. E. Cleasby[1] · C. Chenu[1]

Abstract

Summary In contrast to previously reported elevations in serum sclerostin levels in diabetic patients, the present study shows that the impaired bone microarchitecture and cellular turnover associated with type 2 diabetes mellitus (T2DM)-like conditions in ZDF rats are not correlated with changes in serum and bone sclerostin expression.

Introduction T2DM is associated with impaired skeletal structure and a higher prevalence of bone fractures. Sclerostin, a negative regulator of bone formation, is elevated in serum of diabetic patients. We aimed to relate changes in bone architecture and cellular activities to sclerostin production in the Zucker diabetic fatty (ZDF) rat.

Methods Bone density and architecture were measured by micro-CT and bone remodelling by histomorphometry in tibiae and femurs of 14-week-old male ZDF rats and lean Zucker controls ($n = 6$/group).

Results ZDF rats showed lower trabecular bone mineral density and bone mass compared to controls, due to decreases in bone volume and thickness, along with impaired bone connectivity and cortical bone geometry. Bone remodelling was impaired in diabetic rats, demonstrated by decreased bone formation rate and increased percentage of tartrate-resistant acid phosphatase-positive osteoclastic surfaces. Serum sclerostin levels (ELISA) were higher in ZDF compared to lean rats at 9 weeks (+40 %, $p < 0.01$), but this difference disappeared as their glucose control deteriorated and by week 14, ZDF rats had lower sclerostin levels than control rats (−44 %, $p < 0.0001$). Bone sclerostin mRNA (qPCR) and protein (immunohistochemistry) were similar in ZDF, and lean rats at 14 weeks and genotype did not affect the number of empty osteocytic lacunae in cortical and trabecular bone.

Conclusion T2DM results in impaired skeletal architecture through altered remodelling pathways, but despite altered serum levels, it does not appear that sclerostin contributes to the deleterious effect of T2DM in rat bone.

Keywords Bone · Sclerostin · Type 2 diabetes · Zucker rats

✉ M. Pereira
  mpereira@rvc.ac.uk

1 Department of Comparative Biomedical sciences, Royal Veterinary College, Royal College Street, London NW1 0TU, UK

2 University College London, London, UK

3 University College Hospital, London, UK

4 The University of Adelaide, Adelaide, Australia

5 Kings College London, London, UK

6 INSERM UMR1033 and Université de Lyon, Lyon, France

Introduction

Type 2 diabetes mellitus (T2DM) is a developing pandemic and an important cause of morbidity and mortality. One major complication of T2DM is a greater risk of bone fractures, leading to a decreased quality of life for patients [1]. Moreover, fracture healing is delayed and accompanied by a higher risk of complications such as infections, non-unions or mal-unions [2]. Clinical evidence indicates that despite patients typically possessing normal or higher bone mineral density (BMD), diabetic bone is more fragile and of poorer quality [3]. There are multiple pathways by which T2DM affects bone quality. For example, the accumulation of advanced glycation end products (AGEs) in bone because of chronic hyperglycaemia can result in altered collagen cross-linking, leading to impairment of mechanical properties and reduced bone strength in diabetic patients [4]. In addition, endocrine

cross-talk between pancreatic β-cells, fat and bone is also thought to be important in the pathogenesis of T2DM [5]. Specifically, osteoblasts have been shown to be insulin targets, with impaired bone formation being a consequence of insulin deficiency in T2DM [6]. However, other pathogenic mechanisms are also thought to be present which contribute to the impaired skeletal strength in T2DM.

Cellular and molecular communication between bone cells is essential to ensure appropriate bone remodelling, which is crucial for optimal skeletal integrity. One of the most important molecular pathways in bone homeostasis is the Wnt signalling pathway, which is essential for bone formation. A major regulator of the Wnt pathway is the product of the SOST gene, sclerostin, which is expressed almost exclusively in osteocytes and acts as a potent inhibitor of bone formation [7]. It can bind to bone morphogenetic proteins (BMPs) and low-density lipoprotein receptor-related proteins 5 and 6 (LRP5/6), inhibiting canonical Wnt/β-catenin signalling, which is essential for osteoblast activity and bone formation and is dysregulated in diabetic patients [8, 9]. Recent studies have shown that circulating sclerostin is elevated in diabetic patients compared to control subjects [10, 11], while serum sclerostin and bone expression levels are also increased in type 1 streptozotocin-induced diabetic rat and type 2 aged Otsuka Long Evans Tokushima Fatty (OLETF) diabetic rats [8, 12]. Conversely, the number of sclerostin-positive osteocytes was decreased in bone from diabetic mice, because of a reduction in osteocyte viability [9]. Recently, it was shown that treatment with a neutralising antibody targeting sclerostin reverses the adverse effect of T2DM on bone mass and strength and improves bone regeneration in rats [13]. However, it is unknown whether an increase in sclerostin production by osteocytes is involved in the pathogenesis of the increased skeletal fragility in diabetic patients.

Previous in vitro work suggests that high glucose concentrations alter the mineralisation process in osteoblasts via decreased calcium uptake [14]. A study in osteocyte-like cells showed that a combination of high glucose and the resulting accumulation of advanced glycation end products (AGEs) suppress bone formation, likely by increasing sclerostin expression [15]. However, it remains unclear exactly how a high glucose environment affects osteocytes and whether altered sclerostin production is a feature.

The skeletal effects of diabetes in laboratory animals have been investigated in various rodent models, including genetic and spontaneously diabetic models that undergo a dynamic period of disease progression. Of these models, the male Zucker diabetic fatty (ZDF) fa/fa rat is widely used. These rats possess a mutation in the gene encoding the leptin receptor, resulting in obesity and subsequent spontaneous development of T2DM-like clinical signs, including early hyperlipidaemia and hyperinsulinaemia, followed by persistent hyperglycaemia and decreased insulin secretion, as a result of pancreatic β-cell

failure [16]. Research on the effects of leptin in bone has yielded inconsistent results, illustrated by the absence of leptin signalling in rodents resulting in an increase [17], a decrease [18] or no change [19] in bone mass. In terms of skeletal characteristics, the ZDF rat has been well studied. Compared to controls, diabetic ZDF rats exhibit shorter femoral length, reduced bone formation, decreases in cortical and trabecular bone mass, and diminished BMD [13, 20–23].

In this study, we aimed to characterise the effects of diabetes on bone architectural and cellular activities in the ZDF rat model and to correlate any changes with sclerostin expression by osteocytes in situ and serum sclerostin concentration. To explore the mechanisms further, we also aimed to examine the effect of high glucose concentrations on bone mineralisation and sclerostin expression by osteoblasts and osteocytes in vitro.

Materials and methods

Animals and study design

Male ZDF rats (ZDF-Lepr[fa]) and Zucker lean rats (ZDF-Crl) ($n = 6$/group) were purchased from Charles River laboratories (Margate, UK) at 8 weeks of age. Rats were acclimatised to their housing (21 °C ± 1 °C; 12 h day/night cycle) for 1 week and fed a high-fat-carbohydrate chow (Purina 5008) (Lab Diet, USA) ad lib. From week 9, rats were weighed weekly and blood glucose was measured weekly using a glucometer (Accuchek Aviva, Roche Diagnostics, Burgess Hill, UK), to identify the onset of frank diabetes. Blood samples were collected at weeks 9, 11, 13 and 14 for measurement of serum sclerostin. To measure bone formation rate in trabecular bone, rats were intraperitoneally injected with calcein (10 mg/kg) and alizarin red complexone (15 mg/kg) (Sigma-Aldrich), respectively 10 and 3 days prior to euthanasia. At week 14, rats were sacrificed; right tibiae were dissected for micro-CT analysis and left tibiae for immunohistochemistry, while right femurs were snap frozen for RNA extraction and left femurs embedded for bone histomorphometry. All animal procedures were approved by the Royal Veterinary College's Ethics and Welfare committee and were carried out under UK Home Office licence to comply with the Animals (scientific procedures) Act 1986 (PPL: 70/7859).

Micro-CT analysis of tibiae

Right tibiae were fixed in 10 % neutral-buffered formalin for 24–48 h and stored in 70 % ethanol at 4 °C. The microarchitecture, BMD for trabecular bone and tissue mineral density (TMD) for cortical bone were then evaluated using high-resolution micro-computed tomography (micro-CT) (10 μm/pixel, 55 kV, 181 μA skyScan-1172/F Bruker,

Kontich, Belgium). Whole tibiae were reconstructed using NRecon version 1.6.9.8 (NRecon®), trabecular and cortical bone areas were analysed with CT-Analyser (CTAn) version 1.14.4.1 and bone structure was quantified using the built-in 2D and 3D analysis software BATMAN v.1.14.4.1. The threshold values for the micro-CT analysis of trabecular bone were chosen to be between 60 and 255 and between 100 and 255 for cortical bone. For analysis of trabecular bone in proximal metaphysis, the 1.5 % of bone length below the appearance of secondary spongiosum was left unanalysed and the 5 % of length following was analysed. The cortical shell was excluded by operator-drawn regions of interest, and 3D algorithms were used to determine the relevant parameters, which included bone volume percentage (BV/TV), trabecular thickness (Tb.Th), trabecular number (Tb.N), structure model index (SMI), trabecular pattern factor (Tb.Pf), trabecular separation (Tb.Sp) and degree of anisotropy (DA). Analysis of cortical bone in midshaft diaphysis was performed using a 0.49-mm-long segment (or 100 tomograms) at 50 % of tibial length from its proximal end. Cortical bone parameters consisted of tissue area (Tt.Ar), tissue perimeter (Tt.Pm), bone area (Ct.Ar), eccentricity (Ecc), cross-sectional thickness (Ct.Th) and maximum moment of inertia (Imax), a parameter used to predict an object's ability to resist torsion.

Bone indentation

Following micro-CT analysis, right tibiae were embedded in methyl methacrylate (MMA) in order to perform microhardness tests. Microhardness is a measurement of the ability of a material's surface to resist indentation with or without permanent indentation on a microstructural scale. Mean bone tissue microhardness was measured using a Micromet 5104 (Buehler, Lake Bluff, Illinois, USA) equipped with a Vickers indenter. Ten transverse indentations were performed at 1.1 cm below the growth plate for all embedded bones. A load of 25 g was applied onto the region of interest for 10 s, which formed a square-based diamond indentation mark. Vickers microhardness (Hv), defined as the mean pressure the material will support under load (expressed in kg/mm^2), was calculated from the equation $Hv = 1854.4 \times P/d^2$, where P is the test load in grammes and d is the mean length of the two diagonals, expressed in millimetre. The data obtained for each bone sample were expressed as a mean of 10 indentations.

Bone histomorphometry

Left femurs were fixed in 4 % formaldehyde for 2 days at 4 °C, dehydrated in acetone for 24 h and embedded in MMA at low temperature to preserve enzymatic activity. Unstained 8-μm-thick longitudinal sections were used for fluorescence microscopy to assess mineral apposition rate (MAR, μm/day). The area of mineralising surfaces was expressed as a ratio of alizarin red-labelled surfaces to total bone surfaces (MS/BS, %) and mineral apposition rate (MAR, μm/day), measured as the average distance between calcein and alizarin red, divided by the number of days elapsed between the administration of such labels (7 days). The bone formation rate was calculated as MS/BS × MAR (BFR/BS, μm^3/μm^2/day). Alternatively, sections were stained for tartrate-resistant acid phosphatase (TRAP) (Leucognost® SP; Merck, Germany) and counterstained with Mayer's haematoxylin solution to visualise osteoclasts in trabecular bone, or stained with Goldner's stain to quantify trabecular microarchitecture parameters within the sections. Histomorphometric parameters were measured in the trabecular bone of the metaphysis, using a region of interest of 2 mm width, below the growth plate. Measurements were performed using image analysis software (Explora Nova, La Rochelle, France). Histomorphometric parameters were reported in accordance with the American Society for Bone and Mineral Research Committee nomenclature.

Histology

Left tibiae of ZDF and lean rats were harvested immediately after sacrifice and fixed in 10 % neutral-buffered formalin for 1 day. All tibiae were subjected to 17 days of decalcification in 14 % ethylenediaminetetraacetic acid (EDTA) at pH 7.4. Tibiae were then embedded in paraffin and sectioned at 5 μm.

Counting the number of empty lacunae

Five sections representing the whole proximal tibial width were stained with haematoxylin and eosin (H&E) to quantify the number of empty osteocytic lacunae in three regions: cortical bone in the diaphysis and trabecular bone in the metaphysis and epiphysis. Five images for each region of each bone (n = 6/group) were acquired using light microscopy. All lacunae in each region were manually counted using dot-counting morphometry (image J) in order to establish the ratio of empty lacunae to total lacunae (an indication of osteocytic death).

Immunohistochemistry for sclerostin

For immunohistochemical labelling, tibial sections were first incubated with 0.1 % trypsin in PBS for 30 min at 37 °C, then washed in 0.025 % Triton in PBS (wash buffer). Endogenous peroxidase activity was blocked using 3 % H$_2$O$_2$ in methanol (30 min) followed by rinsing with wash buffer. The sections were blocked with 3 % BSA in 20 % rabbit serum and then incubated overnight at 4 °C with goat polyclonal anti-mouse sclerostin antibody (10 μg/ml) (AF1589, R&D Systems) and polyclonal goat IgG for control sections (AB-108-C, R&D Systems). Sections were washed and incubated for 30 min in horseradish peroxidase (HRP)-conjugated secondary antibody

(rabbit anti-goat, 1:200) (P0160, Dako). They were then rinsed and HRP-label was visualised by incubating the sections for 5 min with 3,3′ diaminobenzidine (DAB)-solution. Three sections for each bone were counterstained briefly with haematoxylin and imaged using light microscopy to visualise osteocytes within cortical and trabecular bone. All sclerostin-positive osteocytes in bones of ZDF and lean rats were manually counted in these regions using image J.

Number and size of adipocytes

One section of each bone ($n = 6$/group) was stained with H&E to identify adipocytes and images were acquired using bright field microscopy and Leica imaging software. The number and size of adipocytes were measured in the metaphysis. All adipocytes were manually counted in secondary spongiosum using dot-counting morphometry (image J). Adipocyte size was manually drawn and individually measured using image J.

Cell culture

IDG-SW3 cell line

The mouse osteoblastic-late-osteocytic cell line IDG-SW3 was kindly provided by Prof. Linda Bonewald and cultured as previously described [24]. Briefly, cells were cultured in MEM supplemented with 10 % foetal calf serum (FCS), 2 mM L-glutamine, 100 U/ml penicillin and 100 μg/ml streptomycin. Fifty units per millilitre of recombinant mouse interferon-gamma (INF-γ) (Invitrogen) was also added to the cultures to induce expression of the SV40 large tumour antigen and maintain cell proliferation. The IDG-SW3 cells were cultured on rat tail collagen type 1-coated plates (Becton Dickson Bioscience) at 40,000 cells/cm^2 and 33 °C. Osteogenesis was induced at confluence by replacing medium with fresh growth medium supplemented with 50 mg/L ascorbic acid and 4 mM β-glycerophosphate without IFNγ at 37 °C. Cells were maintained for 30 days in osteogenic medium, which was changed three times weekly.

UMR-106 cell line

The rat osteoblastic-like cell line UMR-106 was cultured in Dulbecco's Minimal Essential medium supplemented with 10 % FCS, 2 mM L-glutamine, 100 U/mL penicillin and 100 μg/ml streptomycin at 37 °C for 24 h.

Primary osteoblasts

Primary mouse osteoblastic cells were obtained by sequential enzyme digestion of excised calvarial bones from 2-day-old C57BL/6 mice, using a three-step process (1 % trypsin in PBS for 10 min; 0.2 % collagenase type II in Hanks balanced salt solution (HBSS) for 30 min; 0.2 % collagenase type II in HBSS for 60 min). The first two digests were discarded and the cells resuspended in MEM supplemented with 10 % FCS, 2 mM L-glutamine, 1 % gentamicin, 100 U/ml penicillin, 100 μg/ml streptomycin and 0.25 μg/ml amphotericin. Cells were cultured for 2–4 days at 37 °C in 5 % CO2 until they reached confluence. They were then cultured in six-well trays in MEM supplemented with 2 mM β-glycerophosphate and 50 μg/ml ascorbic acid, with half medium changes every 3 days. Bone nodule formation by osteoblasts was measured after 28 days of culture.

Incubation of cells with high glucose concentrations

IDG-SW3 and UMR 106 cells were cultured with four different concentrations of glucose in six-well plates, using one plate for each. Glucose was added to the medium so that the first concentration mimicked normal the glucose concentration in humans (5.5 mM), the second group represented postprandial levels (11 mM), the third group represented uncontrolled diabetes (22 mM) and the fourth the very high glucose typical of ZDF rats (44 mM). Primary osteoblasts were cultured in low and high glucose conditions (5.5 and 22 mM). IDG-SW3 cells and primary osteoblasts were cultured for 30 days, with supernatants being collected at the end of the experiment. After termination of the experiment, the cells were fixed with 4 % paraformaldehyde for 10 min and stained for mineralisation with alizarin red. Cell layers were imaged at 800 dpi using a high-resolution flat-bed scanner. Binary images of each individual well were then subjected to automated analysis (image J), using constant "threshold" and "minimum particle" levels, to determine the surface area of mineralised bone nodules.

UMR-106 cells were cultured in the four glucose concentrations for 48 h and the supernatant collected. Trypsin was then added to the UMR-106 cells for 5 min at 37 °C to detach them for RNA extraction.

Quantitative PCR

Right femurs were centrifuged at 10.000 rpm to remove the bone marrow and then individually powdered with a mortar and pestle under liquid nitrogen. Total RNA from bones was extracted using TRIzol® reagent or RNeasy Mini Kit (Qiagen) according to the manufacturers' protocols. RNA concentration and purity were estimated by measurement of absorbance at 260 and 280 nm, respectively, and RNA integrity by visualisation of ribosomal bands after agarose gel electrophoresis.

The messenger RNA (mRNA) expression level for *SOST* was determined in control and diabetic bones, as well as in UMR-106 cells. Transcripts were amplified by real-time

quantitative RT-PCR (qPCR) using SYBR GREEN PCR master mix (Qiagen) in a 25 µL reaction volume. Amplification parameters consisted of initial denaturation at 50 °C for 10 min to allow reverse transcription, then 95 °C for initial denaturation and 35 cycles of one-step PCR (denaturation at 95 °C for 10 s, annealing and extension at 60 °C for 30 s) using primer pairs with the following sequences: *SOST*: 5′-GAGTACCCAGAGCCTCCTCA-3′ and 5′-AGCA CACCAACTCGGTGAC-3′, *GAPDH*: 5′-CTCA ACTACATGGTCTACATGT-3′ and 5′-CTTC CCATTCTCAGCCTTGACT-3′ (designed using Blast). Their relative abundance in duplicate cDNA aliquots was quantified using a standard curve plotted from amplification of a 10-fold dilution series of DNA generated by conventional PCR from the same primer pairs and gel purified. Results are quoted after normalisation to expression of GADPH, which was unchanged by the treatments. Generation of a single appropriate PCR product was confirmed by melting curve analysis and periodic agarose gel electrophoresis.

Quantification of sclerostin

Sclerostin levels in rat serum and in the supernatants of UMR-106, primary osteoblasts and IDG-SW3 cells were quantified using a Solid Phase Sandwich ELISA (Mouse/Rat SOST kit, R&D Systems Europe, Ltd., Abingdon, UK) according to the manufacturer's recommendations.

Statistics

Data are presented as mean ± SD. Statistical analyses were conducted using GraphPad Prism® (v. 6.01 for Windows; GraphPad Software Inc., USA). Comparisons between diabetic and lean rats were performed using unpaired *t* tests. Multiple comparisons for in vitro studies were performed using one-way analysis of variance, with Dunnett's post hoc test where appropriate. Other multiple comparisons were performed using a two-way analysis of variance using the Sidak post hoc test where appropriate. $P < 0.05$ was considered to be statistically significant. The in vitro results shown are representative of three independent experiments.

Results

Body weight and blood glucose levels in Zucker diabetic rats

Development of diabetes in ZDF rats was monitored by weekly measurements of body weight and blood glucose levels. Body weights of ZDF rats were higher compared to lean rats at all time points ($p < 0.0001$). However, this difference tended

to disappear as the rats became more diabetic, with values reaching 237 g for lean rats and 312 g for ZDF rats at 9 weeks and 327 g for lean rats and 362 g for ZDF rats at 14 weeks. Furthermore, ZDF rats exhibited dramatically elevated levels of blood glucose compared to controls, with values of 24.8 and 7.8 mmol/L, respectively, at 9 weeks (2.2-fold higher ($p < 0.0001$)) and 30.6 and 7.1 mmol/L, respectively, at 14 weeks (3.3-fold higher ($p < 0.0001$)). These data confirm the expected impairment of glycaemic control in ZDF rats.

Effect of diabetes on bone mineral density, trabecular and cortical bone mass and architecture in ZDF rats

We examined bone mass and architecture in ZDF rats and lean control rats. ZDF rats exhibited a lower tibial bone length (4.7 %, $p < 0.001$) compared with lean rats (Table 1). Trabecular BMD was also lower in the ZDF rats (by 22.2 %, $p < 0.01$) compared with lean rats, while cortical TMD was not different (Table 1). ZDF rats exhibited lower trabecular bone mass, demonstrated by decreased BV/TV and Tb.Th (18.7 %, $p < 0.001$ and 11.7 %, $p < 0.0001$, respectively), compared to the lean controls. They also exhibited impaired connectivity, manifested by a substantial increase in Tb.Pf (91.1 %, $p < 0.05$). There was no significant effect of diabetes on Tb.Sp, Tb.N, SMI or DA (Table 1). Bone histomorphometry measurements in trabecular bone using Goldner staining suggested similarly lower trabecular bone mass in diabetic rats, indicated by lower in BV/TV, Tb.Th and Tb.N (43.4 % ($p < 0.001$), 26.2 % ($p < 0.01$) and 23.8 % ($p < 0.05$), respectively) in ZDF rats compared to lean controls. The separation between trabeculae was increased by 59 % ($p < 0.05$) in ZDF rats, although this was not observed using micro-CT measurements (Table 1).

Consistent with trabecular bone changes, cortical bone geometry was also abnormal in ZDF rats. Analysis half-way along the bone length showed reductions in cortical area and perimeter, illustrated by lower Tt.Ar, Tt.Pm, Ct.Ar (12.7 % ($p < 0.01$), 7.6 % ($p < 0.01$) and 15.5 % ($p < 0.01$), respectively) in ZDF rats compared to lean rats. Imax and Ecc were, respectively, 28.6 % ($p < 0.01$) and 4.3 % ($p < 0.05$) lower in ZDF rats, suggesting that diabetic bone may have reduced strength. Furthermore, transverse bone sections revealed a decrease in Ct.Th of the cortical wall by 7.9 % ($p < 0.01$) in ZDF rats (Table 1).

Effect of diabetes on cortical bone microhardness in ZDF rats

To examine the relationship between bone structure and its mechanical resistance to forces, microhardness tests were performed on cortical bone. No significant difference was observed between the microhardness of cortical bone in ZDF rats (53.94 ± 3.02 kg/mm2) compared to controls

Table 1 Micro-CT and histomorphometric measurements of trabecular and cortical bone architecture in 14-week-old ZDF and Zucker lean rats

Parameters	Zucker lean rats	ZDF rats
Length of tibia (mm)	38.7 ± 0.7	36.9 ± 0.5[***]
Trabecular architecture		
BV/TV (%)	16.95 ± 1.17	13.78 ± 1.08[***]
Tb.Th (mm)	0.0992 ± 0.0019	0.0875 ± 0.0027[****]
Tb.N (number/mm)	1.708 ± 0.103	1.574 ± 0.125
Tb.Pf (factor/mm)	−2.888 ± 2.207	−0.257 ± 1.132[*]
Tb.Sp (mm)	0.932 ± 0.037	0.899 ± 0.038
SMI	1.037 ± 0.166	1.194 ± 0.077
DA	2.166 ± 0.126	2.151 ± 0.082
BMD (g/cm^3)	−0.0011 ± 0.0115	−0.0262 ± 0.0134
Cortical architecture at 50 %		
Tt.Ar (mm^2)	5.90 ± 0.30	5.14 ± 0.43[**]
Tt.Pm (mm)	9.77 ± 0.30	9.03 ± 0.39[**]
Ct.Ar (mm^2)	4.51 ± 0.20	3.81 ± 0.31[**]
Ecc	0.731 ± 0.015	0.699 ± 0.020[*]
I max (mm^4)	3.96 ± 0.42	2.83 ± 0.44[**]
Ct.Th (mm)	0.587 ± 0.017	0.541 ± 0.024[**]
TMD (g/cm^3)	1.270 ± 0.015	1.277 ± 0.013
Trabecular architecture with histomorphometry		
BV/TV (%)	25.43 ± 3.04	14.40 ± 4.04[***]
Tb.Th (mm)	0.0640 ± 0.0078	0.0472 ± 0.0063[**]
Tb.N (number/mm)	3.978 ± 0.260	3.033 ± 0.712[*]
Tb.Sp (mm)	0.188 ± 0.017	0.299 ± 0.090[*]

Measurements were either made in the proximal tibial metaphysis of ZDF rats and Zucker lean rats using micro-CT or in sections of the proximal femoral metaphysis sections using histomorphometry. Measurements of cortical architecture were made using micro-CT in the tibial midshaft diaphysis of ZDF and Zucker lean rats. Mean ± SD of n=6 rats/group

BV/TV bone volume percent, *Tb.N* trabecular number, *Tb.Pf* trabecular pattern factor, *Tb.Th* trabecular thickness, *Tb.Sp* trabecular separation, *SMI* structure model index, *DA* degree of anisotropy, *Tt.Ar* tissue area, *Tt.Pm* tissue perimeter, *Ct.Ar* bone area, *Ecc* eccentricity, *I max* maximal moment of inertia, *Ct.Th* cross-sectional thickness

*P<0.05; **P<0.01; ***P<0.001; ****P<0.0001 versus lean controls

(54.30 ± 2.58 kg/mm^2) ($p = 0.8318$), suggesting that the structural integrity of ZDF cortical bone is maintained (data not shown).

Effect of diabetes on bone turnover

We next examined whether bone remodelling is affected by diabetes. Bone histomorphometry showed uncoupling of bone remodelling in ZDF rats, as there was a substantially increased percentage of TRAP-positive osteoclastic surfaces (108.9 % higher; $p < 0.05$) compared to lean rats (Fig. 1a). Analysis of bone formation activities showed that MAR and BFR were lower in ZDF rats compared to lean rats (by 61.8 %, $p < 0.0001$ and 69.6 %, $p < 0.001$, respectively; Fig. 1b, c).

Effect of diabetes on serum sclerostin levels

Serum sclerostin levels in ZDF and lean rats were assessed by ELISA. At 9 weeks of age, sclerostin levels were 39.8 % higher ($p < 0.01$) in ZDF compared to lean rats. However, this difference disappeared at 11 and 13 weeks, as glycaemic control deteriorates, with sclerostin levels ultimately being 43.5 % lower ($p < 0.0001$) in ZDF than lean rats at 14 weeks of age (Fig. 2a).

Effect of diabetes on numbers of sclerostin-secreting osteocytes and *SOST* mRNA levels

We quantified the number of sclerostin-positive osteocytes in epiphyseal, cortical and trabecular bone using immunohistochemistry and qPCR (Fig. 2c). No significant differences were identified in the number of sclerostin-positive osteocytes in any of these regions between 14-week-old ZDF and lean rats (Fig. 2d). Similarly, no difference was observed in sclerostin mRNA levels in bone between ZDF and lean rats at this age, indicating that sclerostin levels in serum do not reflect current expression levels in bone (Fig. 2b).

Effect of diabetes on the number of empty osteocytic lacunae and adipocytes in ZDF rats

To establish whether diabetes could reduce osteocyte viability, we quantified the number of empty osteocytic lacunae in epiphyseal, cortical and trabecular bone (Fig. 3a). The number of dead osteocytes was similar between ZDF and lean rats in cortical, trabecular and epiphyseal regions (Fig. 3b).

The effect of diabetes on the number and size of adipocytes was also investigated (Fig. 3c). There was no difference in adipocyte number between diabetic and lean rats (Fig. 3d), but adipocyte size was increased by 68 % ($p < 0.0001$) in ZDF rats compared to lean rats (Fig. 3e).

Effect of high glucose concentrations on sclerostin production and mineralisation by osteoblastic and osteocytic cells

To establish whether hyperglycaemia is a key factor mediating the observed effects of diabetes on bone in ZDF rats, we examined the effect of high glucose concentrations on sclerostin production by the UMR osteoblastic cell line and primary osteoblasts. Sclerostin production by UMR-106 cells was increased by 59 % ($p < 0.0001$) and 79.1 % ($p < 0.0001$) in the presence of 22 and 44 mM glucose, respectively (Fig. 4a). Similarly, sclerostin mRNA expression increased in parallel with glucose concentrations (11 mM (+59.3 %), 22 mM (+181 %) and 44 mM (+246.2 %)) (Fig. 4b). In contrast, sclerostin production by primary osteoblasts was not affected by high glucose concentrations (Fig. 4d). We could
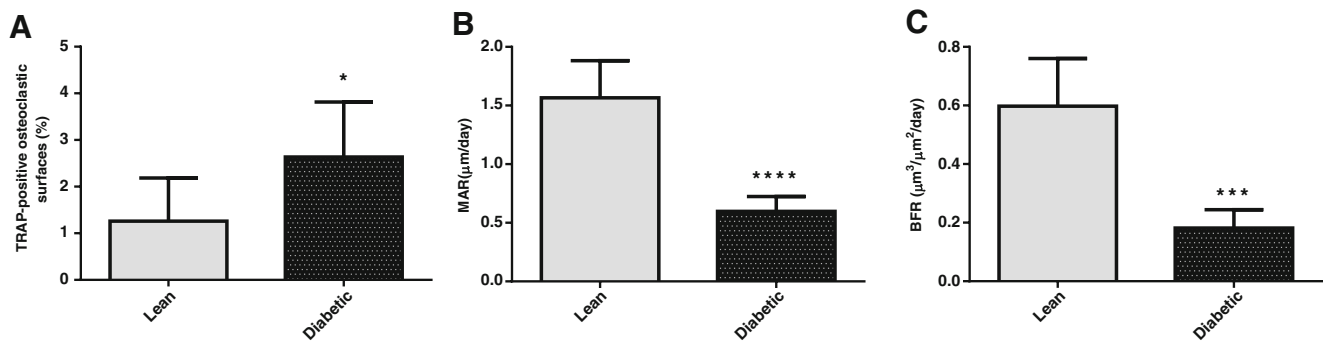
Fig. 1 Bone turnover parameters measured by bone histomorphometry in ZDF and non-diabetic Zucker rats. Measurements were performed by bone histomorphometry on trabecular femoral sections of 14-week-old ZDF and lean rats. **a** Osteoclastic surfaces per millimetre of trabecular bone surface: *TRAP Oc·S/BS*. **b** Mineral apposition rate: *MAR*. **c** Bone formation rate: *BFR*. *Bars* represent mean ± SD of $n = 6$ rats/group. *$P < 0.05$, ***$P < 0.001$, ****$P < 0.0001$ versus control

not detect sclerostin mRNA and protein expression in IDG-SW3 cells after analysis at various cell passage numbers. However, in this cell line, high glucose concentrations impaired mineralisation, as glucose concentrations of 11, 22 and 44 mM decreased mineralisation by 14.9 % ($p < 0.01$), 26 % ($p < 0.0001$) and 24.5 % ($p < 0.0001$), respectively (Fig. 4c). Similarly, bone nodule formation by primary osteoblasts was reduced by 81 % ($p < 0.0001$) in the presence of a high glucose concentration (Fig. 4e).

Discussion

This study is novel in two regards. Firstly, in the use of a rat model of T2DM to investigate the effects of diabetes on bone structural properties and turnover in parallel with bone sclerostin expression levels and osteocyte viability and secondly, in modelling the effect of hyperglycaemia on matrix mineralisation and sclerostin production in osteoblasts and osteocytes in vitro. We demonstrate that ZDF rats have
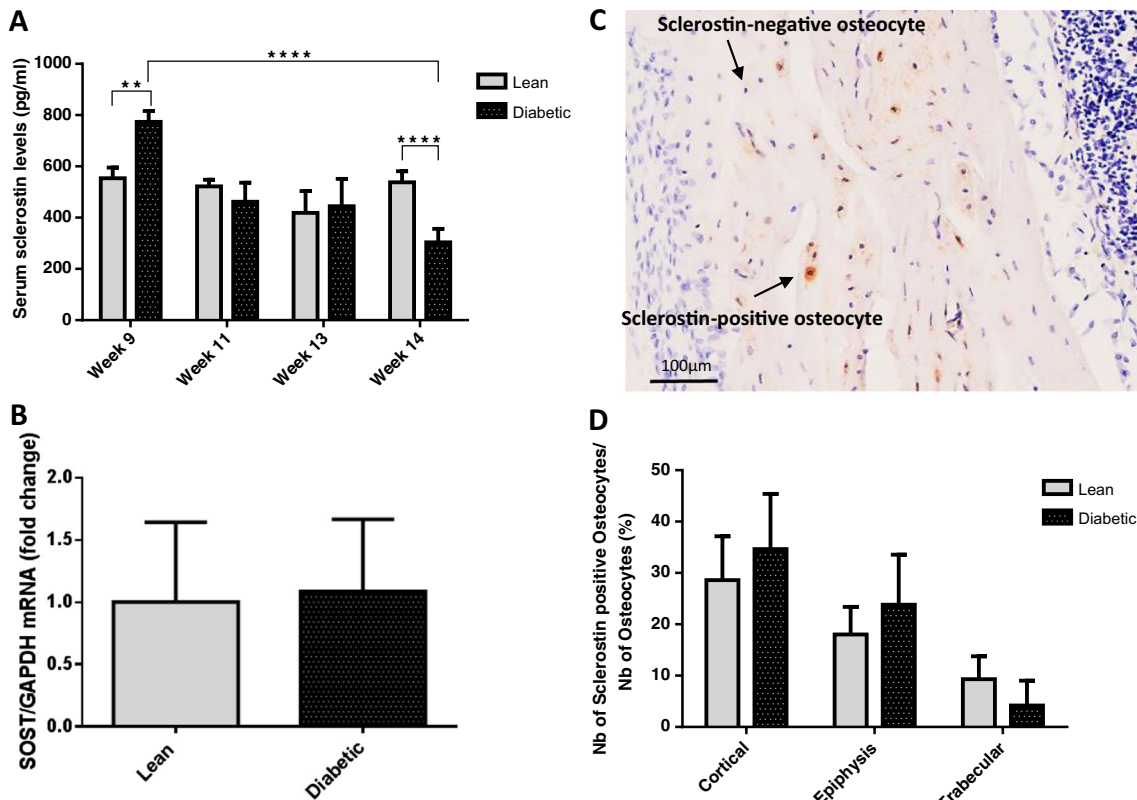

Fig. 2 Serum and bone sclerostin levels in ZDF and control Zucker rats. **a** Serum sclerostin levels at 9 and 14 weeks of age, measured by ELISA. **b** Bone sclerostin mRNA expression normalised to *GAPDH*, quantified by qPCR. **c** Representative longitudinal section of the cortical metaphysis region of the tibiae in which quantification was performed. **d** Ratio of number of sclerostin-positive osteocytes to total number of osteocytes, assessed using immunohistochemistry. *Bars* represent mean ± SD of $n = 6$ rats/group. **$P < 0.01$, ****$P < 0.0001$ versus control
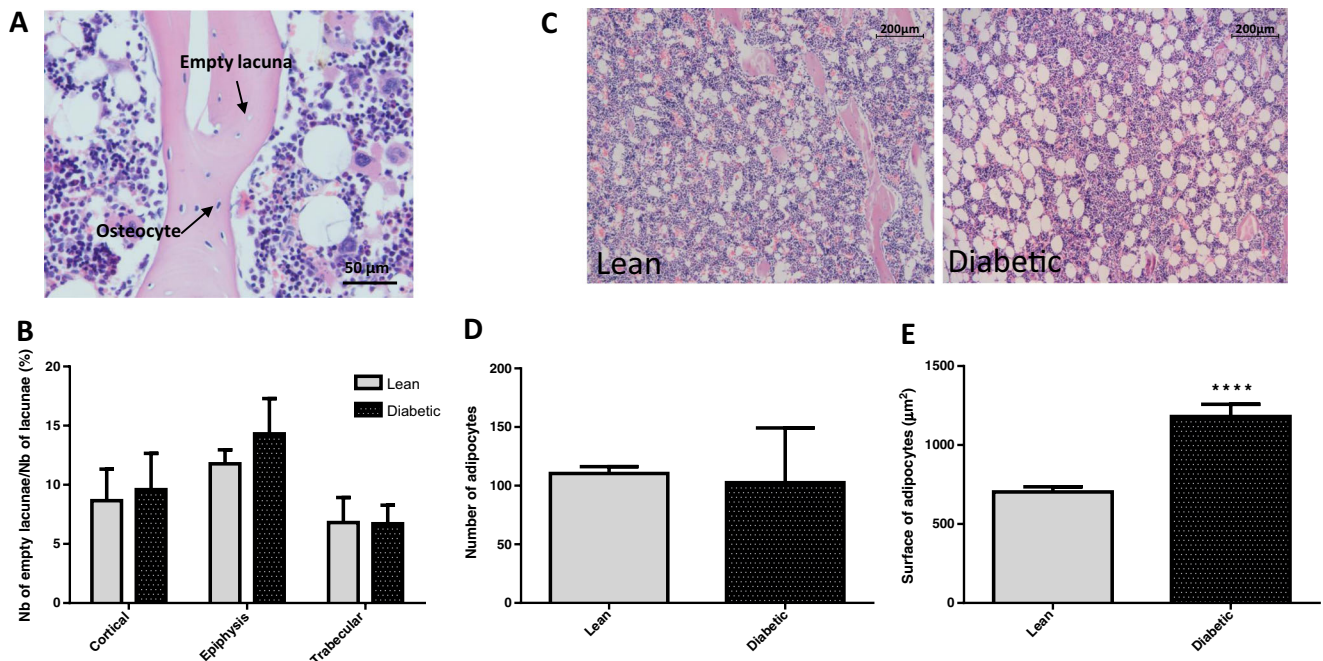
Fig. 3 Bone histology in ZDF and non-diabetic Zucker rats. **a** Representative haematoxylin-eosin staining of tibiae showing the empty osteocytic lacunae and osteocytes within the trabecular bone. **b** Ratio between number of empty osteocytic lacunae/ total number of lacunae. **c** Representative haematoxylin-eosin staining of tibiae along with the distribution of adipocytes in lean (left) and ZDF rats (right). **d** Number of adipocytes. **e** Surface of adipocytes. *Bars* represent mean ± SD of $n = 6$ rats/group. ****$P < 0.0001$ versus control
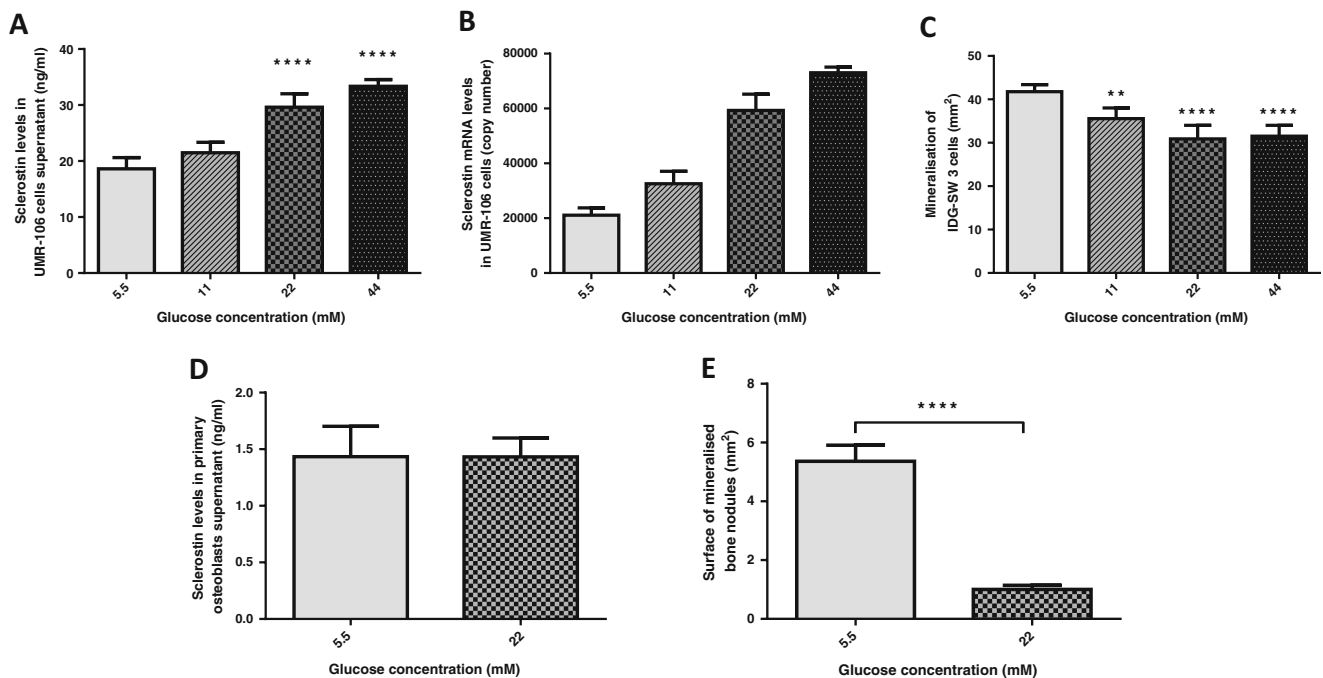

Fig. 4 Effects of high glucose concentrations on sclerostin production by UMR 106 cells and primary osteoblasts and in vitro mineralisation of IDG-SW3 cells and primary osteoblasts. UMR-106 cells and IDG-SW3 were cultured in various glucose concentrations (5.5, 11, 22 and 44 mM) while primary osteoblasts were cultured in only two concentrations (5.5, 22 mM). **a** Sclerostin levels measured in the supernatant of UMR-106 cells by ELISA. **b** Sclerostin mRNA expression in UMR-106 cells, measured using qPCR. **c** Quantification of mineralisation by IDG-SW3 cells after 30 days of culture. **d** Sclerostin levels measured in the supernatant of primary osteoblasts by ELISA. **e** Quantification of mineralisation by primary osteoblasts after 4 weeks of culture. *Bars* represent mean ± SD of $n = 6$ wells/group. **$P < 0.01$, ****$P < 0.0001$ versus control. Experiments were carried out in triplicate, except for primary osteoblasts, in which one experiment was performed

abnormal bone architecture, associated with lower bone re-modelling. Although high glucose concentrations led to an increase in sclerostin production by UMR-106 osteoblastic cells, this effect was not replicated in primary osteoblasts. Furthermore, bone sclerostin levels and the number of viable osteocytes were unchanged in diabetic bone, implying that altered sclerostin levels might not be indicative of impaired bone structure in diabetic rats.

We used a well-established rodent model of T2DM that progressively develops the typical pathology of and shares a number of common metabolic disturbances with human patients, including the insulin resistance, hyperglycaemia and hyperinsulinaemia [21]. ZDF rats showed highly abnormal glucose control at 14 weeks of age. Diabetes also impaired bone mass, evidenced by a decrease in trabecular bone volume, because of reductions in trabecular thickness and impaired connectivity. Cortical bone was similarly affected, as it exhibited significantly reduced cortical bone area and thickness and the suggested resistance to torsion implies reduced bone strength if the materials properties are similar. These results are in agreement with other investigations that demonstrated impaired bone mass and strength in ZDF rats after onset of overt diabetic symptoms [13, 20–23], and they collectively confirm that T2DM adversely affects trabecular microarchitecture and cortical bone geometry. However, the micro-CT analysis showed significantly lower trabecular, but not cortical, BMD in ZDF rats, which contrasts with the phenotype of diabetic patients, who usually have normal or higher BMD [3]. Considering the impaired bone structural properties and Imax, we would also expect lower mechanical resistance and strength, but our results demonstrate that microhardness of cortical bone was unchanged in diabetic rats. However, microhardness relates mostly to the degree of cortical bone mineralisation rather than the arrangement of collagen fibres [25]. In diabetic rats, it is likely that changes in mechanical properties are mainly caused by collagen cross-linking, following the production of AGEs with hyperglycaemia [26]. Hence, as microhardness mainly relates to the mineral component of bone, and cortical mineral density was not affected, these data may not accurately reflect the changes in bone strength in diabetic bone that have been previously shown in the literature using a technique such as three-point bending, which specifically measures bone strength [21].

The deleterious effects of diabetes on bone mass and architecture were confirmed in histological sections using bone histomorphometry. Consistent with the decreases in trabecular and cortical bone mass, histomorphometric evaluation of trabecular bone cellular activities showed significantly uncoupled bone remodelling in diabetic bone, illustrated by increased osteoclast surfaces combined with decreased mineral apposition rate and bone formation rate. The observed reduction in bone formation in ZDF rats is consistent with the results of previously published studies [13, 27]. Although, previous studies of the effect of diabetes on bone resorption have shown no difference in bone resorption between ZDF diabetic and control rats [28] or increased bone resorption in ZDF rats [18], the results of most studies performed in other diabetic rodent models are consistent with ours [29, 30].

Various mechanisms may explain the architectural changes observed in diabetic bone. In addition to decreased leptin levels [22], hyperglycaemia is a possible cause of skeletal deterioration in diabetic ZDF rats [21, 23]. It has been shown that hyperglycaemia can trigger oxidative stress, resulting in alteration of bone architecture [31]. Moreover, hyperglycaemia and the resulting excessive formation of AGEs have been suggested to exert a deleterious skeletal effect by increasing stiffness of the collagen network and suppressing in vitro bone formation [32]. Although we were not able to assess the formation of AGEs in bone in this study, it is likely that ZDF rats had increased skeletal levels of AGEs [33], which would impair osteoblastic cell function through modification of type I collagen. This would be consistent with the observed increase in osteoclast surfaces, since AGEs were shown to enhance osteoclast maturation and function [34]. Therefore, the microarchitectural deterioration of bone in the diabetic rats may partly be a consequence of the accumulation of AGEs. Recent evidence suggests that a combination of hyperglycaemia and AGEs suppresses bone formation and inhibits bone matrix mineralisation by increasing sclerostin expression in osteocyte-like MLO-Y4-A2 cells [15]. It has been suggested that high glucose concentrations stimulate sclerostin secretion in osteoblastic and osteocytic cell lines. Consistent with previous data, our results show increased sclerostin production in UMR-106 cells with increasing glucose concentrations, implying a stimulatory effect of hyperglycaemia on sclerostin production [35, 36]. However, we could not detect sclerostin expression in the osteocytic cell line IDG-SW3 at any stage of differentiation, suggesting that IDG-SW3 cells might not be suitable for the study of sclerostin expression. Exposure of osteocytic IDG-SW3 cells to high glucose levels inhibited in vitro mineralisation in a concentration-dependent manner. These findings are in agreement with previous in vitro studies showing that high glucose concentrations impair calcium deposition and decrease mineralisation in osteoblast cultures [14, 37], independently of an increase in sclerostin.

In addition to the observed deleterious effect of T2DM on bone mass and architecture, this study clearly demonstrates that diabetes decreases bone formation. Several studies have identified impaired bone formation as a consequence of suppressed osteoblastogenesis, based on reduced expression of bone formation markers such as osteocalcin and Runx2 [8, 13, 20]. As the Wnt signalling pathway is crucial for bone formation and regulates the expression of Runx2, it has been suggested that diabetes decreases osteoblastogenesis through the inhibition of Wnt signalling [8]. Based on the inhibitory action of sclerostin on Wnt signalling, we anticipated that sclerostin expression levels would be elevated in diabetic rats,

potentially causing the impaired osteoblastogenesis. In accordance with clinical studies on T2DM patients [10, 11], 9-week-old ZDF rats had increased circulating levels of sclerostin. However, this difference disappeared as the rats got older and glucose control deteriorated still further, ultimately resulting in lower serum sclerostin levels in the diabetic rats at 14 weeks of age. Thus, it could be that sclerostin levels in serum correlate better with the degree of glucose control remaining or the age of the rats, rather than the presence or absence of diabetes. Sclerostin levels greatly increase with age in mice and humans [38, 39], thus it seems unlikely that age contributes to the decrease in sclerostin levels observed in our study at 14 weeks of age. However, we cannot exclude that the lower bone mass observed in ZDF rats at 14 weeks may imply the presence of fewer osteocytes and consequently reduced sclerostin release into the serum of diabetic rats.

Several studies in humans and mice have revealed that serum sclerostin levels do not necessarily reflect contemporaneous differences in the local production of sclerostin in bone [40, 41]. Due to this inconsistency between serum sclerostin and bone mRNA expression, we investigated sclerostin expression levels in bone at both the mRNA and protein levels. We found no differences in bone sclerostin mRNA expression and the number of sclerostin-positive osteocytes between ZDF and control rats. One possible limitation could be the technique used to assess protein levels, as immunohistochemistry allows the enumeration of sclerostin-secreting osteocytes, but does not quantify the level of sclerostin produced per osteocyte. In contrast, results from a previous study [8] showed that in streptozotocin-induced diabetic rats, a model for T1DM, there was increased expression of sclerostin mRNA in bone. This discrepancy could be due to the diabetic model used and suggests that sclerostin levels in bone may be increased in T1DM rats but not in T2DM. However, in another murine model of T1DM, there was a down-regulation of sclerostin mRNA levels in bone, which was ascribed to increased osteocyte apoptosis [9]. In addition, in our study, there was no difference in the number of empty osteocyte lacunae between ZDF and control groups, implying no change in osteocyte viability. Thus, our data collectively indicate that the alterations in microarchitecture and bone turnover associated with T2DM-like conditions in ZDF rats are not a consequence of elevated sclerostin expression and that in this model sclerostin levels in serum do not correlate with its expression in bone.

Significantly, Roforth et al. [41] suggested that circulating sclerostin is derived from several other non-skeletal sources, as well as from articular cartilage chondrocytes [39], and all this information combined implies that measurement of serum sclerostin may not be useful as a predictive biomarker for impaired bone formation. Serum sclerostin levels have been measured in many clinical conditions and consistent changes were not always observed [42], suggesting the need for a better understanding of the factors that control sclerostin production by osteocytes and possibly more consistent serum sclerostin assays. Our in vitro data also suggest that sclerostin levels in bone cell supernatants do not always correlate with bone formation and glucose levels, as an increase in sclerostin production was observed in UMR 106 osteoblastic cells when cultured with high glucose concentration, while this was not confirmed in primary osteoblasts, which express low levels of sclerostin. Similarly, although the osteocytic cell line IDG-SW3 was previously shown to produce sclerostin mRNA and protein with differentiation [24], we and others have found no sclerostin expression in this cell line, despite analysis at various cell passage numbers. The cause of this discrepancy is unclear but could be due to immunoassay variability.

As the altered bone turnover observed in the diabetic rats could neither be explained by a sclerostin-mediated inhibition of Wnt signalling pathway, nor by a reduction in osteocyte viability, we examined whether impaired osteoblastic differentiation could be at fault, which would be indicated by increased numbers of adipocytes. Bone marrow mesenchymal stem cells (BMMSCs) have the ability to differentiate into various cell types, including osteoblasts and adipocytes. Obesity and diabetes are associated with bone marrow adiposity and increased production of tumour necrosis factor-α (TNF-α), an inflammatory cytokine that suppresses osteoblastogenesis and mineralisation [43]. We hypothesised that BMMSCs may have differentiated into adipocytes rather than osteoblasts and, their differentiation being crucial for bone remodelling [44], this could contribute to the decreased BFR observed in the diabetic rats. Obesity and T2DM are characterised by an elevated fat mass, mainly resulting from hypertrophy, rather than hyperplasia of adipocytes [45]. Consistent with this, ZDF rat adipocytes were larger than controls, but there was no difference in the number of adipocytes within the bone marrow. Nevertheless, the enlarged adipocytes observed in diabetic conditions might be another mediator of the observed skeletal fragility.

In conclusion, this is the first extensive study to examine the role of sclerostin in the pathogenesis of T2DM using ZDF rats. Taken together, our results demonstrate that T2DM has a deleterious effect on trabecular bone architecture and cortical bone geometry due to lower bone formation and higher bone resorption. However, our data indicate that the alterations in microarchitecture and bone turnover associated with T2DM-like conditions in ZDF rats are not a consequence of elevated sclerostin expression. As T2DM likely affects bones via multiple mechanisms, further studies are warranted to elucidate the various factors that account for the increased bone fragility observed in T2DM patients.

References

1. Yamamoto M, Yamaguchi T, Yamauchi M, Kaji H, Sugimoto T (2009) Diabetic patients have an increased risk of vertebral fractures independent of BMD or diabetic complications. J Bone Miner Res Off J Am Soc Bone Miner Res 24:702–709

2. Loder RT (1988) The influence of diabetes mellitus on the healing of closed fractures. Clinical orthopaedics and related research 210–216

3. Vestergaard P (2007) Discrepancies in bone mineral density and fracture risk in patients with type 1 and type 2 diabetes—a meta-analysis. Osteoporos Int: J Established Result Cooperation Between Eur Found Osteoporos Natl Osteoporos Found USA 18:427–444

4. Katayama Y, Akatsu T, Yamamoto M, Kugai N, Nagata N (1996) Role of nonenzymatic glycosylation of type I collagen in diabetic osteopenia. J Bone Miner Res Off J Am Soc Bone Miner Res 11:931–937

5. Lecka-Czernik B (2008) Local and systemic functions of bone fat and its contribution to the energy metabolism—the effect of diabetes and obesity on bone. J Musculoskelet Neuronal Interact 8:346–347

6. Clemens TL, Karsenty G (2011) The osteoblast: an insulin target cell controlling glucose homeostasis. J Bone Miner Res Off J Am Soc Bone Miner Res 26:677–680

7. Li X, Ominsky MS, Niu QT, et al. (2008) Targeted deletion of the sclerostin gene in mice results in increased bone formation and bone strength. J Bone Miner Res Off J Am Soc Bone Miner Res 23:860–869

8. Hie M, Iitsuka N, Otsuka T, Tsukamoto I (2011) Insulin-dependent diabetes mellitus decreases osteoblastogenesis associated with the inhibition of Wnt signaling through increased expression of Sost and Dkk1 and inhibition of Akt activation. Int J Mol Med 28:455–462

9. Portal-Nunez S, Lozano D, de Castro LF, de Gortazar AR, Nogues X, Esbrit P (2010) Alterations of the Wnt/beta-catenin pathway and its target genes for the N- and C-terminal domains of parathyroid hormone-related protein in bone from diabetic mice. FEBS Lett 584:3095–3100

10. Gennari L, Merlotti D, Valenti R, et al. (2012) Circulating sclerostin levels and bone turnover in type 1 and type 2 diabetes. J Clin Endocrinol Metab 97:1737–1744

11. Garcia-Martin A, Rozas-Moreno P, Reyes-Garcia R, Morales-Santana S, Garcia-Fontana B, Garcia-Salcedo JA, Munoz-Torres M (2012) Circulating levels of sclerostin are increased in patients with type 2 diabetes mellitus. J Clin Endocrinol Metab 97:234–241

12. Kim JY, Lee SK, Jo KJ, Song DY, Lim DM, Park KY, Bonewald LF, Kim BJ (2013) Exendin-4 increases bone mineral density in type 2 diabetic OLETF rats potentially through the down-regulation of SOST/sclerostin in osteocytes. Life Sci 92:533–540

13. Hamann C, Rauner M, Hohna Y, et al. (2013) Sclerostin antibody treatment improves bone mass, bone strength, and bone defect regeneration in rats with type 2 diabetes mellitus. J Bone Miner Res Off J Am Soc Bone Miner Res 28:627–638

14. Balint E, Szabo P, Marshall CF, Sprague SM (2001) Glucose-induced inhibition of in vitro bone mineralization. Bone 28:21–28

15. Tanaka K, Yamaguchi T, Kanazawa I, Sugimoto T (2015) Effects of high glucose and advanced glycation end products on the expressions of sclerostin and RANKL as well as apoptosis in osteocyte-like MLO-Y4-A2 cells. Biochem Biophys Res Commun 461:193–199

16. Yokoi N, Hoshino M, Hidaka S, Yoshida E, Beppu M, Hoshikawa R, Sudo K, Kawada A, Takagi S, Seino S (2013) A novel rat model of type 2 diabetes: the Zucker fatty diabetes mellitus ZFDM rat. J Diabetes Res 2013:103731

17. Takeda S, Elefteriou F, Levasseur R, Liu X, Zhao L, Parker KL, Armstrong D, Ducy P, Karsenty G (2002) Leptin regulates bone formation via the sympathetic nervous system. Cell 111:305–317

18. Tamasi JA, Arey BJ, Bertolini DR, Feyen JH (2003) Characterization of bone structure in leptin receptor-deficient Zucker (fa/fa) rats. J Bone Miner Res Off J Am Soc Bone Miner Res 18:1605–1611

19. Unger RH, Zhou YT, Orci L (1999) Regulation of fatty acid homeostasis in cells: novel role of leptin. Proc Natl Acad Sci U S A 96:2327–2332

20. Hamann C, Goettsch C, Mettelsiefen J, et al. (2011) Delayed bone regeneration and low bone mass in a rat model of insulin-resistant type 2 diabetes mellitus is due to impaired osteoblast function. Am J Phys Endocrinol Metab 301:E1220–E1228

21. Reinwald S, Peterson RG, Allen MR, Burr DB (2009) Skeletal changes associated with the onset of type 2 diabetes in the ZDF and ZDSD rodent models. Am J Phys Endocrinol Metab 296:E765–E774

22. Liu Z, Aronson J, Wahl EC, Liu L, Perrien DS, Kern PA, Fowlkes JL, Thrailkill KM, Bunn RC, Cockrell GE, Skinner RA, Lumpkin CK, Jr. (2007) A novel rat model for the study of deficits in bone formation in type-2 diabetes. Acta Orthop 78(1):46–55

23. Prisby RD, Swift JM, Bloomfield SA, Hogan HA, Delp MD (2008) Altered bone mass, geometry and mechanical properties during the development and progression of type 2 diabetes in the Zucker diabetic fatty rat. J Endocrinol 199:379–388

24. Woo SM, Rosser J, Dusevich V, Kalajzic I, Bonewald LF (2011) Cell line IDG-SW3 replicates osteoblast-to-late-osteocyte differentiation in vitro and accelerates bone formation in vivo. J Bone Miner Res Off J Am Soc Bone Miner Res 26:2634–2646

25. Feagin F, Koulourides T, Pigman W (1969) The characterization of enamel surface demineralization, remineralization, and associated hardness changes in human and bovine material. Arch Oral Biol 14:1407–1417

26. Yamamoto M, Yamaguchi T, Yamauchi M, Sugimoto T (2009) Low serum level of the endogenous secretory receptor for advanced glycation end products (esRAGE) is a risk factor for prevalent vertebral fractures independent of bone mineral density in patients with type 2 diabetes. Diabetes Care 32:2263–2268

27. Picke AK, Gordaliza Alaguero I, Campbell GM, Gluer CC, Salbach-Hirsch J, Rauner M, Hofbauer LC, Hofbauer C (2015) Bone defect regeneration and cortical bone parameters of type 2 diabetic rats are improved by insulin therapy. Bone

28. Liu R, Bal HS, Desta T, Krothapalli N, Alyassi M, Luan Q, Graves DT (2006) Diabetes enhances periodontal bone loss through enhanced resorption and diminished bone formation. J Dent Res 85(6):510–514

29. Mansur SA, Mieczkowska A, Flatt PR, Bouvard B, Chappard D, Irwin N, Mabilleau G (2016) A new stable GIP-Oxyntomodulin hybrid peptide improved bone strength both at the organ and tissue levels in genetically-inherited type 2 diabetes mellitus. Bone 87:102–113

30. Glorie L, Behets GJ, Baerts L, De Meester I, D'Haese PC, Verhulst A (2014) DPP IV inhibitor treatment attenuates bone loss and improves mechanical bone strength in male diabetic rats. Am J Phys Endocrinol Metab 307:E447–E455

31. Hamada Y, Fujii H, Fukagawa M (2009) Role of oxidative stress in diabetic bone disorder. Bone 45(Suppl 1):S35–S38

32. Ogawa N, Yamaguchi T, Yano S, Yamauchi M, Yamamoto M, Sugimoto T (2007) The combination of high glucose and advanced

glycation end-products (AGEs) inhibits the mineralization of osteo-blastic MC3T3-E1 cells through glucose-induced increase in the receptor for AGEs. Hormone and metabolic research = Hormon-und Stoffwechselforschung =. Horm Metab 39:871–875

33. Campbell GM, Tiwari S, Hofbauer C, et al. (2016) Effects of para-thyroid hormone on cortical porosity, non-enzymatic glycation and bone tissue mechanics in rats with type 2 diabetes mellitus. Bone 82:116–121

34. Zhou Z, Immel D, Xi CX, Bierhaus A, Feng X, Mei L, Nawroth P, Stern DM, Xiong WC (2006) Regulation of osteoclast function and bone mass by RAGE. J Exp Med 203:1067–1080

35. Kang J, Boonanantanasarn K, Baek K, Woo KM, Ryoo HM, Baek JH, Kim GS (2015) Hyperglycemia increases the expression levels of sclerostin in a reactive oxygen species- and tumor necrosis factor-alpha-dependent manner. J Periodontal Implant Sci 45:101–110

36. Garcia-Hernandez A, Arzate H, Gil-Chavarria I, Rojo R, Moreno-Fierros L (2012) High glucose concentrations alter the biomineral-ization process in human osteoblastic cells. Bone 50:276–288

37. You L, Gu W, Chen L, Pan L, Chen J, Peng Y (2014) MiR-378 overexpression attenuates high glucose-suppressed osteogenic dif-ferentiation through targeting CASP3 and activating PI3K/Akt sig-naling pathway. Int J Clin Exp Pathol 7:7249–7261

38. Modder UI, Hoey KA, Amin S, McCready LK, Achenbach SJ, Riggs BL, Melton LJ 3rd, Khosla S (2011) Relation of age, gender, and bone mass to circulating sclerostin levels in women and men. J Bone Miner Res Off J Am Soc Bone Miner Res 26:373–379

39. Thompson ML, Jimenez-Andrade JM, Mantyh PW (2016) Sclerostin Immunoreactivity increases in cortical bone osteocytes and decreases in articular cartilage chondrocytes in aging mice. J Histochem Cytochem : Off J Histochem Soc 64:179–189

40. Jastrzebski S, Kalinowski J, Stolina M, Mirza F, Torreggiani E, Kalajzic I, Won HY, Lee SK, Lorenzo J (2013) Changes in bone sclerostin levels in mice after ovariectomy vary independently of changes in serum sclerostin levels. J Bone Miner Res Off J Am Soc Bone Miner Res 28:618–626

41. Roforth MM, Fujita K, McGregor UI, Kirmani S, McCready LK, Peterson JM, Drake MT, Monroe DG, Khosla S (2014) Effects of age on bone mRNA levels of sclerostin and other genes relevant to bone metabolism in humans. Bone 59:1–6

42. Clarke BL, Drake MT (2013) Clinical utility of serum sclerostin measurements. BoneKEy Rep 2:361

43. Chang J, Wang Z, Tang E, Fan Z, McCauley L, Franceschi R, Guan K, Krebsbach PH, Wang CY (2009) Inhibition of osteoblastic bone formation by nuclear factor-nB. Nat Med 15:682–689

44. Crane JL, Cao X (2014) Bone marrow mesenchymal stem cells and TGF-beta signaling in bone remodeling. J Clin Invest 124:466–472

45. Skurk T, Alberti-Huber C, Herder C, Hauner H (2007) Relationship between adipocyte size and adipokine expression and secretion. J Clin Endocrinol Metab 92:1023–1033